Ericsson heat engine with microchannel recuperator for solar concentrator with flat mirrors

Ernst Kussul, Oleksandr Makeyev, Tatiana Baidyk, Jose Saniger Blesa, and Neil Bruce

***Abstract*—** In this article we propose new support frame structure for solar concentrator with flat mirrors, discuss the assembly method of the frame structure, and propose the Ericsson heat engine to transfer the heat energy to electrical energy. At present, Stirling cycle and Rankine cycle heat engines are used to transform the heat energy of solar concentrators to mechanical and electrical energy. The Rankine cycle is used for large-scale solar power plants. The Stirling cycle can be used for small-scale solar power plants. The Stirling cycle heat engine has many advantages such as high efficiency, long service life, silent operation, etc. However, the Stirling cycle is good for high temperature difference (up to 700 C). It demands the use of expensive materials and has problems of lubrication. Its efficiency depends on the efficiency of the heat regenerator. The design and manufacture of a heat regenerator is not a trivial problem because the regenerator has to be placed in the internal space of the engine. It is possible to avoid this problem if we place the regenerator out of the internal engine space. To realize this idea it is necessary to develop the Ericsson cycle heat engine. We propose a structure of this engine. A computer simulation was made to evaluate the Ericsson engine parameters. In this article we discuss the obtained results.

***Keywords*—** flat mirrors, Ericsson cycle heat engine, microchannel recuperator, Rankine heat engines, solar concentrator, Stirling cycle, support frame.

I. Introduction

THE problem of fossil fuel substitution with sustainable energy sources is one of the most important problems of the 21st century [1]. There are many different sources of sustainable energy: solar energy, wind energy, geothermal energy, energy of ocean waves, tidal energy, etc. Indirectly many of them are produced as a result of solar activity, but usually the term “solar energy” means direct transformation of sun light to other types of energy.

There are solar concentrators of different types [2]. The most of them are channel concentrators, concentrator towers and parabolic trough type. Channel concentrators do not allow obtaining a high concentration ratio. Tower type concentrators have a complex control system and are also relatively expensive. Conventional parabolic concentrators are expensive because the parabolic surface is formed of two components: a rigid support and the flexible mirror. The mirrors are made of flexible high-cost special glass.

It was proposed to approximate the parabolic surface with a large amount of spherical mirrors [3]. The price of spherical mirrors is less than the parabolic mirror though still high.

There are concentrators that use a large number of small flat mirrors that approximate a parabolic surface [3] - [7]. The concentrator of this type was developed at Australian National University [6] and used in the solar power plant "White Cliffs" in Australia. The concentrator supporting device having a parabolic shape was made from fiberglass. Over 2,300 flat mirrors of size (100 x 100) mm^2 were glued to the concave surface of this dish.

There are different types of solar energy plants. The two most popular types are Photovoltaic Systems and Solar Thermal Energy Systems (STES). In this work we will consider STES. Normally STES consists of a solar concentrator, a heat engine and a generator of electric current. Sometimes it also includes an energy storage system. The solar concentrator permits us to obtain the high temperature needed for heat engines. In our previous work we described a low-cost solar concentrator based on multiple triangular flat facets [5], [8], [9]. Two prototypes of the solar concentrators are presented in Fig.1.

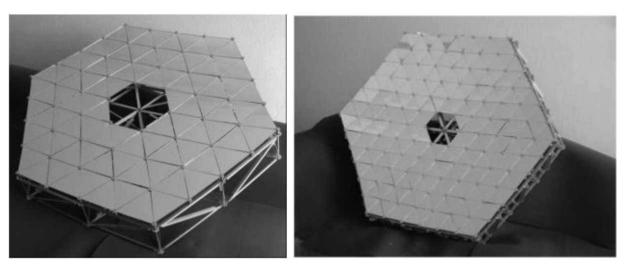

Fig.1. Two prototypes of the solar concentrators

Before describing the Ericsson engine we want to explain the solar concentrator structure.

E. Kussul is with the CCADET, UNAM (National Autonomous University of Mexico), Circuito Exterior s/n, Ciudad Universitaria, 04510, Mexico city, D.F., Mexico (52 55 56228602; fax: 52 55 55500654; e-mail: ekussul@ unam.mx).

O. Makeyev is with University of Rhode Island, USA.

T. Baidyk, J. Saniger and N. Bruce are with the the CCADET, UNAM (National Autonomous University of Mexico), Circuito Exterior s/n, Ciudad Universitaria, 04510, Mexico city, D.F., Mexico (t.baydyk@ccadet.unam.mx).

This work was supported partially by projects PAPIIT IN110510-3, PAPIIT IN119610.

II. Support Frame for Solar Concentrator

In the literature [4], [5], the flat mirror solar concentrator with support frame constructed form bars and nodes was described (Fig.2).

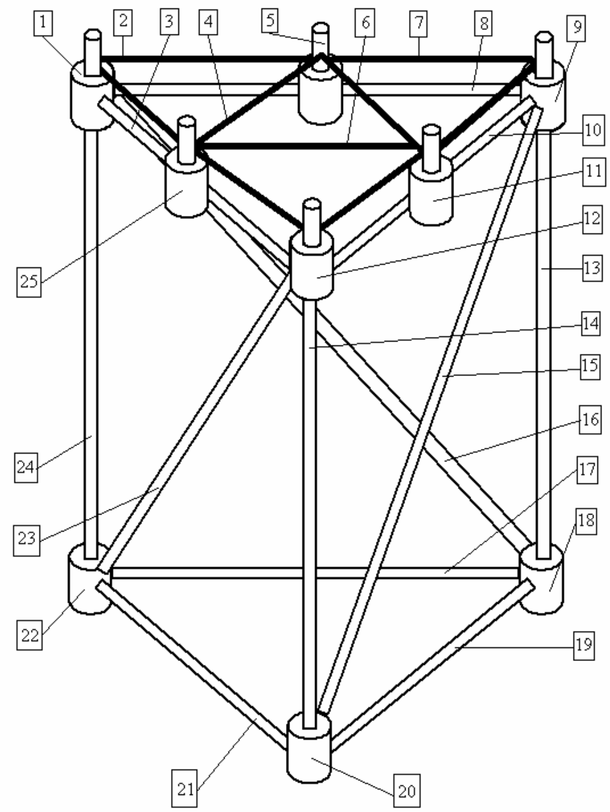

Fig.2. Cell of the solar concentrator support frame

The price of flat mirrors is smaller than the spherical or parabolic mirrors. At present it is about 3 dollars per square meter [10]. There is a concentrator that uses a large number of small flat mirrors that approximate a parabolic surface [4], [5]. This concentrator has a supporting device from bars and nodes (Fig.2).

The disadvantage of this device is that assembly of the support frame is complicated. For example, the supporting frame for 90 flat mirrors contains 144 bars. Fig.3 shows the support frame. To assemble this device is necessary to find the positions of two terminals of each bar and set accessories on these terminals. As shown in Fig.3, the access to some nodes is difficult in assembly process.

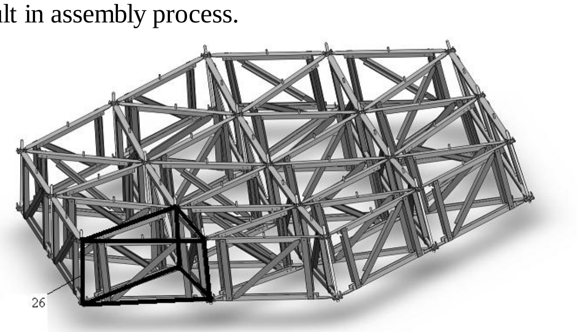

Fig.3. Support frame

Practically, the assembly process is the most expensive stage in manufacturing process of the solar concentrator.

The prototype of the concentrator frame (Fig.3) showed the possibility of obtaining the temperature to 300 degrees centigrade. For the temperature of 450 degrees centigrade it is necessary to make the prototype that contains 210 flat mirrors. This device will have 288 bars and 576 nodes for bar unions. In this case the assembly process is very costly.

We propose to facilitate the assembly process using preassembled modules. Two types of pre-assembled modules are shown in Fig. 4 and 5. The module of the first type is shown in Fig.4.

Fig.4. First type module

The module of the second type (vertical bar) shown in Fig.5, it has two nodes: top node (Fig.6) and bottom node (Fig.7). These nodes are used to join the modules of the first type. The cell of solar concentrator support frame is presented in Fig.8.

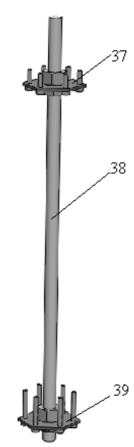

Fig.5. Module of the second type (vertical bar)

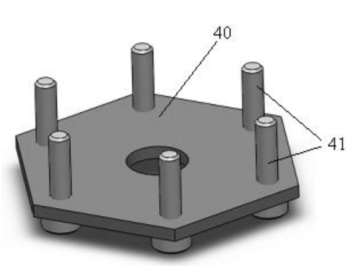

Fig.6. Top node

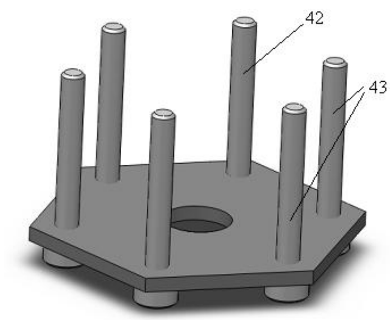

Fig.7. Bottom node

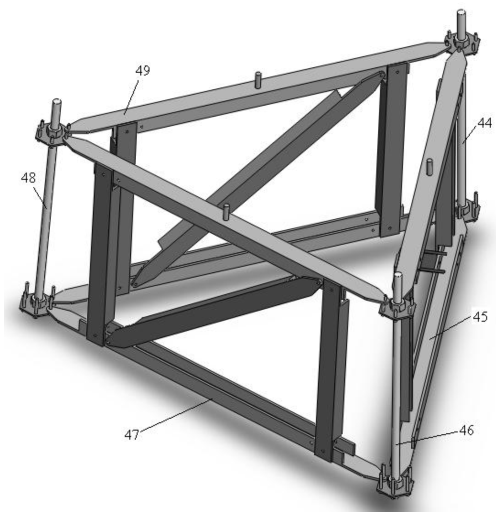

Fig.8. Cell of solar concentrator support frame

III. Support Frame Manufacture

We produced the prototype of this solar concentrator support frame. Two prototypes of solar concentrators are presented in Fig.1.

Solar concentrators with flat mirrors can have a low cost because the flat mirrors are mass produced with standard technology and every square meter of flat mirrors can cost 20-30 times less than the shaped mirrors.

To obtain the approximation of the parabolic surface the plane mirrors are produced as the triangles with vertices placed in parabolic surface. It was proposed to adjust manually the positions of these vertices.

In the patent [11] it is proposed to adjust the positions of vertices using the special screws. Each screw can move six vertices of the triangles neighbors. It is proposed to focus reflected light using mirrors for position adjustment. This method is very complicated because the movement of one screw affects in parallel to six neighboring mirrors. To make adjustment of all mirrors it is really necessary to solve many linear equations explicitly, or to use many sequential trials.

It was also proposed another method of adjusting flat mirrors [12]. In this design each mirror has two rotational axes and mirror position adjustment is proposed to do manually using reflected beam of light. In this case the adjustment of the mirror does not influence the positions of other mirrors and this simplifies the process of adjustment. The disadvantage of this method is that manual adjustment of the position of each mirror is labor costly.

In the patent [13] we proposed to use the parabolic gauge that turns on the support structure (Fig.9) to adjust the parabolic surface of solar concentrator.

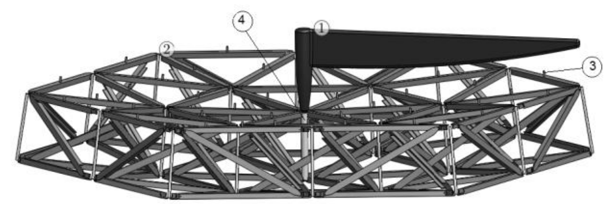

Fig.9. Manual setting the parabolic surface of support frame with the parabolic gauge

The support system with adjustment device of parabolic surface is shown in Fig.9.

The support system contains the bar structure, parabolic gauge 1, the central tube 4, distance screw 3, the nuts for adjusting parabolic surface 2.

The process of adjusting parabolic surface consists of the following steps:

1. The gauge 1 of the adjustment device is placed inside the central tube 4.
2. Gauge 1 is turned on until at least one unadjusted nut will be below the parabolic edge of the gauge.
3. The nut is set up (by turning it on the screw) to make contact with the parabolic edge of the gauge.
4. The position of the nut is fixed with special fixing screw.
5. In case any nut still is not adjusted repeat steps 2-4.
6. If all the nuts have been adjusted terminate the process and eliminate the gauge of the central tube.

The disadvantage of this method is use of manual labor in the process of adjustment.

The rotation of the gauge (step 2) and adjusting the positions of the nuts (step 3) can be done with the robot arm controlled by computer vision.

The device is based on stereoscopic computer vision (Fig.10).

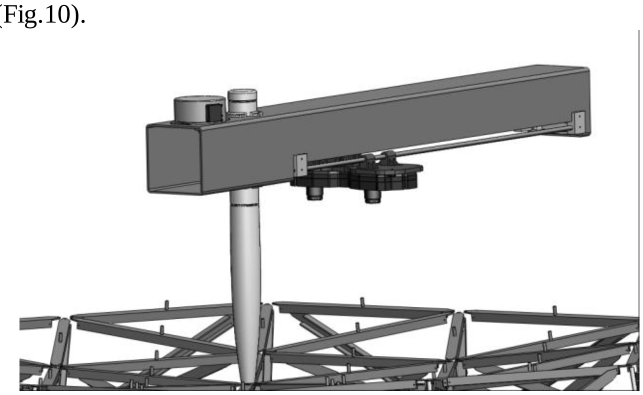

Fig.10. Stereoscopic computer vision system for structure adjustment

In this device we propose to replace the parabolic gauge with a robot arm (Fig.11) that has the axis 5 and is installed at the central tube so that it can rotate the nuts 4 around the screws 3 to adjust nuts positions. The robot arm has a carriage 9 which can move in radial direction using two parallel guides 11. This carriage has two web cameras 10 for stereo vision and telescopic tube 12 to rotate the adjusting nuts relatively the screws 4.

To adjust the parabolic surface the device makes the following steps:

1. automatically finds the nut 4 that is not adjusted;
2. Place the telescopic tube on this nut;
3. Move down the telescopic tube 12 to contact with nut 4;
4. Connect the head (Fig. 12) with nut 4;
5. Rotate the telescopic tube 12 with the nut 4 to the position corresponding to the parabolic surface. This position is obtained from two webcams with stereo vision algorithm;
6. Disconnect the telescopic tube 12 and the nut 4;

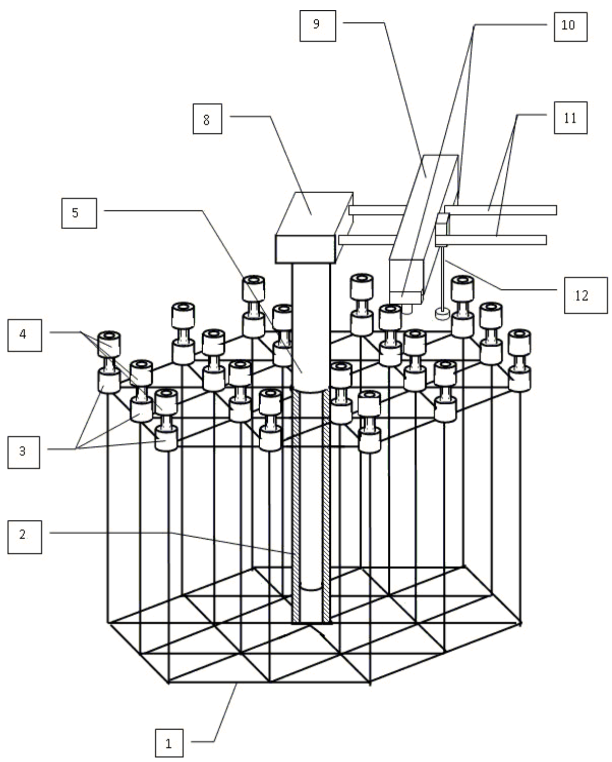

Fig.11. Automatic adjustment device of the parabolic surface

7. Move up the telescopic tube 12;
8. If there are nuts unadjusted repeat the process from 1 to 7. If all the nuts are adjusted the process is terminated.

IV. Heat Engines

The solar concentrator permits us to obtain the high temperature needed for heat engines. In previous sections we described a low-cost solar concentrator based on multiple triangular flat facets. Now we will analyze which type of heat engine is most useful for these solar concentrators.

Two types of heat engines are usually used now in STES: steam turbines and Stirling engines [14] – [17]. Steam turbines are good for large power plants and Stirling engines are proposed for distributed installations.

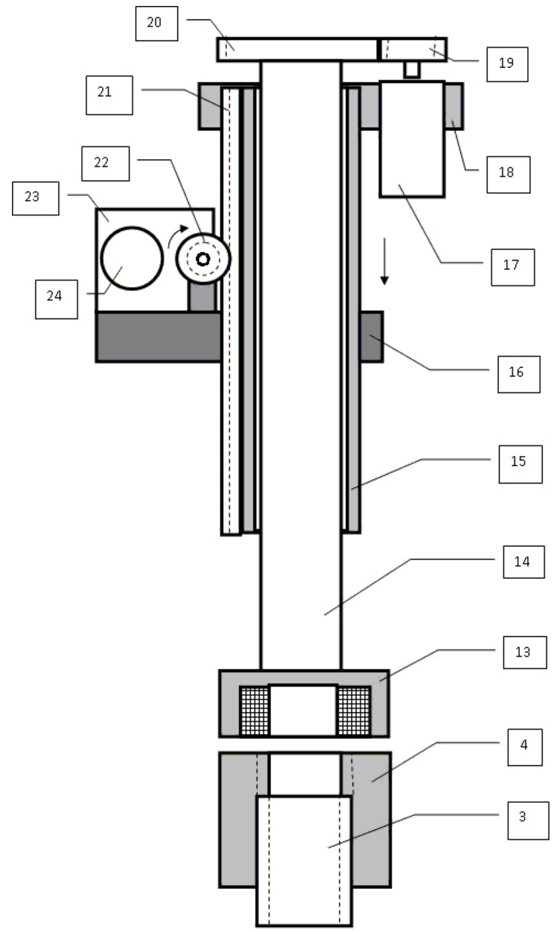

Fig.12. Telescopic tube with electromagnetic head to turn the adjusting nuts

The Stirling engine in general has high efficiency, long service life, and many other useful properties but in existing versions it demands expensive materials and high precision manufacturing. This leads to elevated cost of this engine. Moreover it needs a high concentration ratio of solar concentrators (up to 700 – 1000 suns) that also increases the cost.

The Ericsson Cycle Heat Engine (ECHE) at present is less popular and less investigated than the Stirling Engine but it has many promising peculiarities and can be considered as a good candidate for STES [18], [19], [20].

V. Stirling Heat Engines

As a rule Stirling engines are used to transform thermal energy to electricity. For this purpose Stirling engine is placed to the focal point of solar concentrator. Stirling engines have many advantages but they demand high temperature difference between hot and cold sides of the engine. Therefore they demand high temperature materials that have elevated cost.

One type of Stirling Engine (alpha Stirling Engine) is shown in Fig.13.

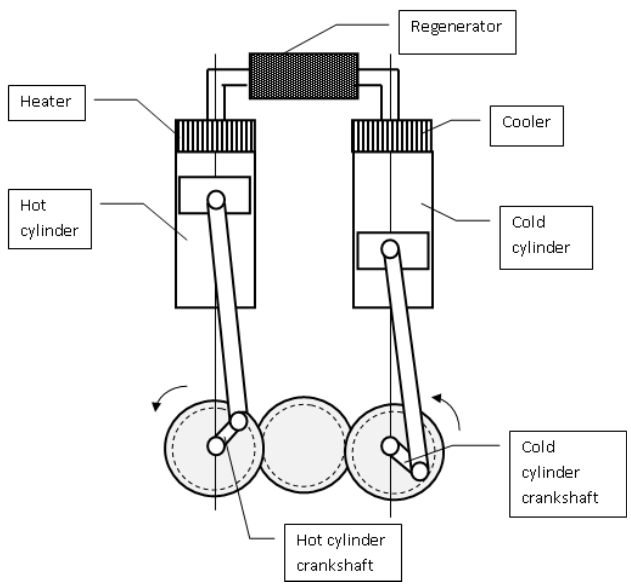

Fig.13. Stirling engine

It contains a hot cylinder, a heater, a regenerator, a cooler, a cold cylinder, and 2 crankshafts that drive the pistons of the hot cylinder and the cold cylinder. The crankshafts are connected to the gears so that the hot cylinder crankshaft is displaced on 90^0 relative to the cold cylinder crankshaft. This displacement ensures the compression of the working liquid (gas) in the cold cylinder. After compression the working liquid is displaced from the cold cylinder to the hot cylinder. In this process the working liquid is heated to the temperature of the heater and hot cylinder. In the hot cylinder the working liquid is expanded and produces more work than was spent during its compression in the cold cylinder. Thereafter the working liquid is moved from the hot cylinder to the cold cylinder.

The Stirling engine has many advantages. It has very long life time, low level of noise, it can be used for small power plants, and it has a simple structure without valves. But the simple structure of the Stirling engine generates many problems. In theory the Stirling cycle consists of the following processes:

- Isothermal compression,
- Heating at constant volume,
- Isothermal expansion,
- Cooling at constant volume.

Real Stirling engines at present have no isothermal processes. To approximate the compression and expansion of the working liquid to the isothermal processes it is necessary to increase the thermal conductivity of working liquid, to decrease the rotation speed of the engine or to decrease the size of the cylinders. To increase the thermal conductivity modern Stirling engines use Hydrogen or Helium instead of air. The thermal conductivity of Helium and Hydrogen is 6-7 times higher than the thermal conductivity of air. However, it is not sufficient to obtain the compression and expansion processes close to the isothermal process. Practically it is impossible to decrease the speed of rotation of the engine to obtain isothermal compression and expansion because in this case the specific power (the relation of the power to the engine weight) drastically decreases. In principle it is possible to obtain isothermal processes if we decrease the sizes and increase the number of the cylinders. A rough estimation shows that it is possible to obtain good approximation to isothermal processes if the engine of 1 kW has about 1 000 000 cylinders of sizes less than 1 mm. At present we have no technology to produce such engines.

At present existing Stirling engines have compression and expansion processes that are closer to adiabatic processes than to isothermal processes. The difference between these processes is small if the compression and expansion rate is small. For example, if the coefficient of compression is 1.1 (10 %), the change of the temperature in adiabatic processes for Hydrogen is less than 3 %, and the process can be considered as quasi-isothermal. Normal engines with small coefficient of compression have low power. To preserve acceptable power the pressure in all the space of the engine is made high (for example 100 bar). In this case the pressure difference is sufficiently large (10 bar) and the engine has acceptable power. These conditions demand the development of a regenerator of very high efficiency. Real regenerators do not permit us to obtain Carnot efficiency (efficiency of an engine divided by efficiency of Carnot cycle) of Stirling engines more than 0.6. For this reason it is necessary to increase the temperature of the hot cylinder to obtain good overall efficiency of the engine. High temperature of the hot cylinder demands the use of special materials that increase the cost of the engine.

VI. Ericsson Heat Engine

There is another method to obtain approximately isothermal processes of compression and expansion. This method is used in some multistage gas turbines where the gas is cooled during the compression stages and is heated during the expansion stages. The method can also be used in piston engines including relatively low-power engines but in piston engines it demands the use of valves and cannot be realized in Stirling engines, but can be realized in Ericsson engine. One example of Ericsson engine is described in [20]. The engine power is 10.8 kW. It is based on the open cycle that is the air from atmosphere enters to the two stage compressor with intermediate cooling. Compressed air enters to the recuperator at the temperature of 146°C at the pressure of 600kPa. In the recuperator it is heated up to 379°C and after that enters to the heater, where its temperature increases to 800°C. With this temperature the air goes to the expander where its temperature drops down to 405°C due to almost adiabatic expansion. After expander the air flows through the recuperator where it is cooled down to 172°C. At this temperature the air goes to the atmosphere.

We propose to use Ericsson engine that can work with much lower temperature difference and has no problems with lubrication. We expect that Ericsson engine will be less expensive than Stirling engine.

The theoretical Ericsson cycle is made up of two isothermal processes and two isobaric processes. As it was mentioned in [20] this theoretical cycle is not appropriate to study Ericsson engine. Really, the theoretical Ericsson cycle demands isothermal expansion of the air and the engine described in [20] has almost adiabatic expansion process were temperature drops from 800°C to 405°C. To improve real Ericsson cycle it is necessary to decrease compression (and expansion) rate from 6 in the mentioned engine to 1.2 - 1.4. With this compression ratio the adiabatic process has small difference from the isothermal process, but in this case the power of the engine will decrease. To restore the engine power it is possible to make a multistage compression with the intermediate cooling and a multistage expansion with intermediate heating [21], [22]. This type of engine is shown in Fig.14. It is possible to increase additionally the engine power if we will use the closed thermal cycle instead of open cycle used in [20]. The closed cycle permits us to increase the total pressure in the engine space. In our example we consider the total pressure equals to 20 bars.

The engine presented in Fig.14 consists of 3 compressors, 3 coolers, 3 expanders, 3 heaters, and recuperator. The number of the compressors, expanders, coolers and heaters can be more than 3. The coolers are placed at the input of each compressor, and the heaters are placed at the input of each expander. The Ericsson engine uses a recuperator instead of the regenerator that is used in the Stirling engine. The recuperator has two areas: the first area contains high pressure gas obtained from the compressors and the second area contains low pressure gas obtained from the expanders.

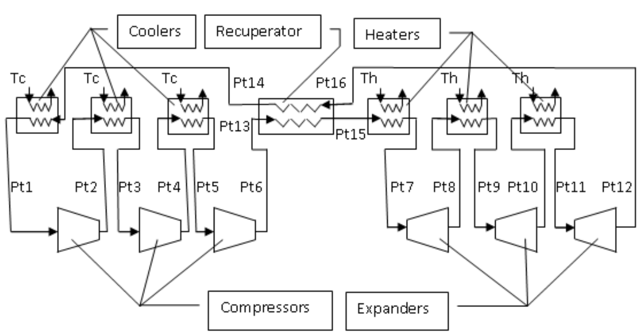

Fig.14. Ericsson engine

The heat exchanger of the recuperator permits heating of the compressed gas using the heat energy of the expanded gas.

The Ericsson engine works as follows: the working gas that is cooled in the recuperator and in the first cooler, is compressed in the first compressor. The compression rate at this stage is as low as in the Stirling engine. The temperature of the gas at the compressor output is slightly higher than the temperature at the compressor input. After the first compressor the gas flows to the cooler that decreases the gas temperature. After that gas flows to the second compressor, where its pressure and temperature increase, but the temperature is returned to its previous value in the third cooler. In principle many stages of compression and cooling may be used to obtain a quasi-isothermal process of compression with high compression rate. A similar process occurs at the expansion of the gas. The difference is that we use expanders instead of compressors and heaters instead of coolers.

The proposed design of the engine permits us to obtain acceptable approximation of isothermal processes preserving high compression and expansion rates and acceptable specific power of the engine.

The scheme (Fig.14) contains the parameters of the gas at the points marked in the scheme as Pt_i. In this scheme p_i means the pressure, T_i means the absolute temperature, and v_i means specific volume of the gas. All the parameters can be calculated using a special program written in the language "C".

The parameters of Ericsson engine were calculated using the program. The results are presented in Table 1 (EV is the engine version, for all versions P_1=20 bar, T_c=273°K, and V_1=0.01 m^3/s).

Table 1. Ericsson engine parameters

EV	λ	T_h (°K)	T_{c1} (°K)	T_{h6} (°K)	$\Delta T_{3\text{-}2}$ (°K)	$\Delta T_{5\text{-}4}$ (°K)	W	η_T	η_C	η_{TC}
1	1.2	573	5	5	10	10	10548	0.43	0.524	0.83
2	1.2	573	3	3	5	5	10783	0.46	0.524	0.88
3	1.4	573	3	3	5	5	18559	0.45	0.524	0.86
4	1.4	453	3	3	5	5	10191	0.31	0.397	0.78
5	1.4	453	5	5	10	10	9827	0.29	0.397	0.73
6	1.2	573	13	13	26	26	9641	0.35	0.524	0.67

In this table p_1 is the pressure of the gas at the input of the first compressor, λ is the compression rate in one compressor or expansion rate in one expander, T_c is the temperature of the cool liquid at the input of Ericsson engine, T_h is the temperature of hot liquid at the input of the Ericsson engine, ΔT_{c1} is the temperature difference between the gas and cooling liquids in the coolers, ΔT_{h6} is the temperature difference between the gas and hot liquids in the heaters, $\Delta T_{3\text{-}2}$ is the temperature difference between the low pressure and the high pressure gas in the recuperator at the compressor side, $\Delta T_{5\text{-}4}$ is the temperature difference between the low pressure and the high pressure gas in the recuperator at the expander side, V_1 is the volumetric gas flow rate at the input of the first compressor, W is the engine power, η_T is the thermal efficiency of the Ericsson engine, η_C is the efficiency of Carnot, η_{TC} is the relation of thermal efficiency of the Ericsson engine to the efficiency of Carnot (in the literature this is termed as Carnot efficiency).

In our case the highest temperature of Ericsson engine is 573°K (300°C). This temperature permits us to use synthetic lubrication oils in all parts of Ericsson engine. Using of lubrication increases the service life and mechanical efficiency of the engine.

To create the Ericsson heat engine it is necessary to implement compressors, expanders, coolers, heaters and recuperator. In this article we describe the design of compressors, expanders and recuperator. All compressors and expanders have the same design shown in Fig.15 but differ in sizes and/or rotation speed.

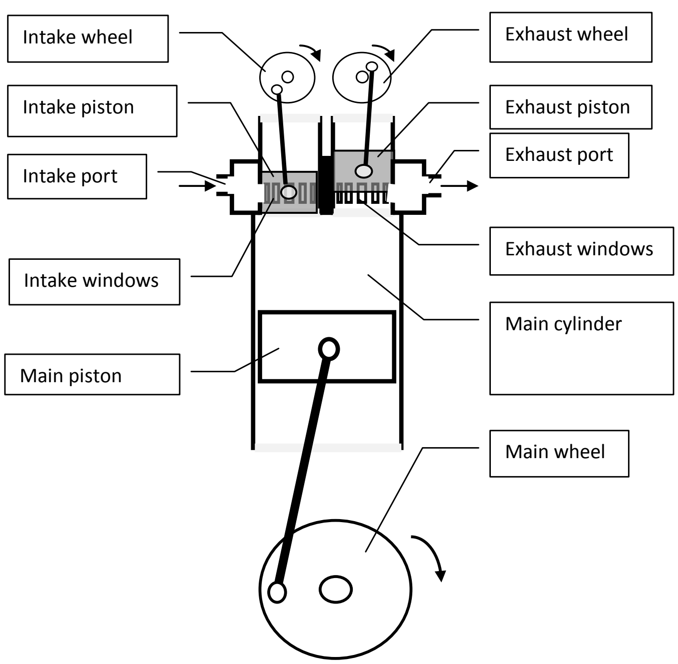

Fig.15. Scheme of compressor/expander for Ericsson heat engine

The intake piston and exhaust piston periodically open and close the intake windows and exhaust windows. The time diagram of compressor windows opening is shown in Fig.16.

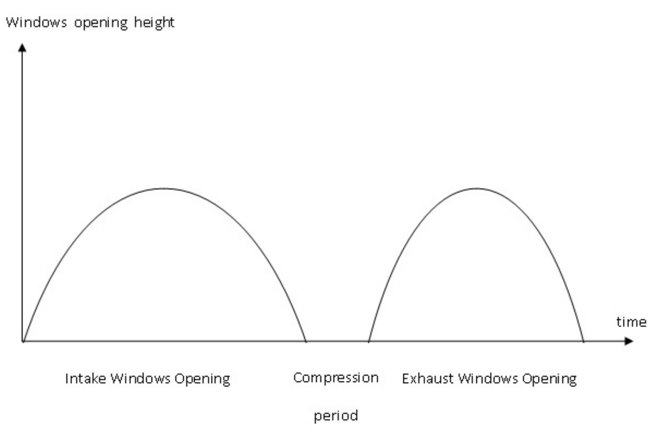

Fig.16 Time diagram of compressor windows opening

In the first period (Intake Windows Opening) the intake windows are opened and exhaust windows are closed. This period lasts half of the whole cycle period. In the next period (Compression period) all windows are closed. This period lasts a small portion of the whole cycle period (10 – 15%). In the third period the exhaust windows are opened and the intake windows are closed. The time diagram of expander windows opening is shown in Fig.17.

In the first part (Intake Windows Opening) the intake windows are opened and exhaust windows are closed. This period approximately lasts 35 – 40% of whole the cycle period. In the next period (Expansion period) all windows are closed. This period lasts 10 – 15% of the whole cycle period. In the third period the exhaust windows are opened and intake windows are closed. This period lasts half of the whole cycle period.

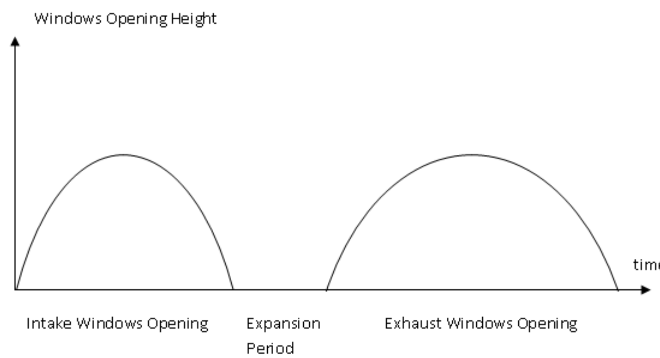

Fig.17 Time diagram of expander windows opening

With these time diagrams the compressor takes the gas from the intake port, slightly compresses it, and pushes the gas through the exhaust port. The expander receives the compressed hot gas from the intake port, allows the gas to expand, and pushes it through exhaust port. Small compression and expansion rate in each main cylinder permits us to consider the process as an isothermal one. In this case all the walls of the cylinders and all pistons will have approximately the same temperature and can be made so precise that they need no piston rings. This will result in high mechanical efficiency.

If we will use the heat exchangers of engine described in [20] with high temperature differences up to 26°C (line 6 in the Table 1) we will obtain low efficiency, η_{TC} = 0.67. To increase this efficiency it is necessary to design a special microchannel heat exchanger that will have the temperature differences indicated in lines 1-5 of Table 1. This heat exchanger is described below.

VII. Microchannel Recuperator

The main element of microchannel recuperator is its base plate (Fig.18). The base plate is circular plate from the metal with high thermal conductivity (copper, aluminum, etc.). This plate contains several circles of holes that form microchannels for compressed and expanded air. Each circle for compressed air (excluding external circle) is located between two circles for expanded air and each circle for expanded air (excluding internal circle) is located between two circles for compressed air. In Fig.18 only two circles are presented. The microchannel recuperator contains many base plates separated by sealing rings (Fig.19) in the manner that each zone of compressed and expanded air is hermetically sealed.

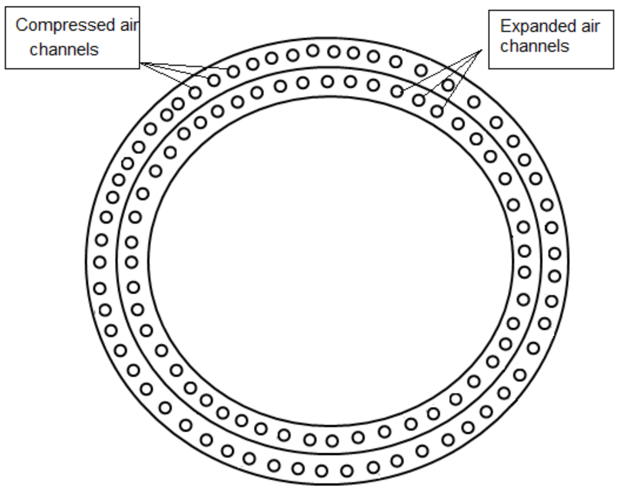

Fig.18. Base plate of microchannel recuperator

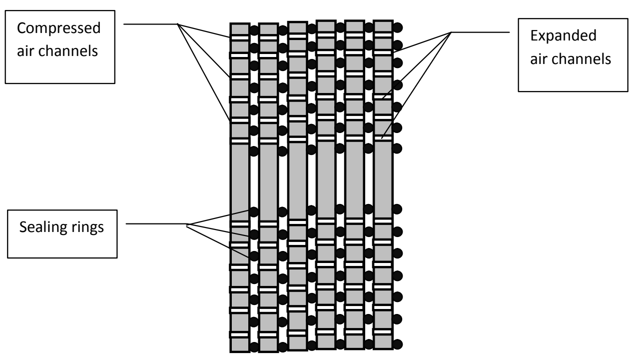

Fig.19. Microchannel recuperator design

In Fig.20 we present the fragment of microchannel recuperator.

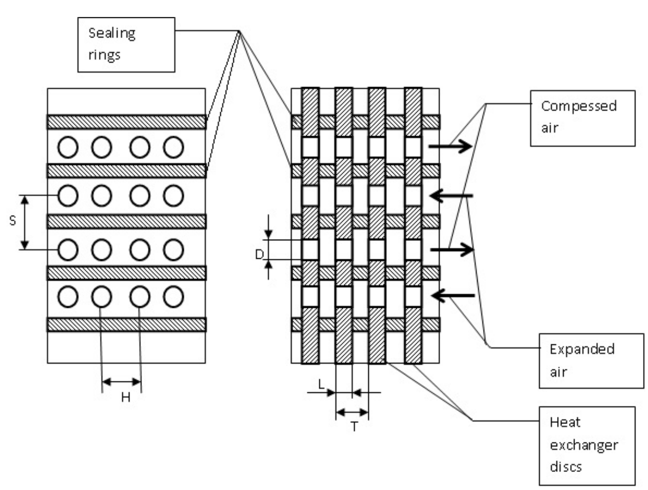

Fig.20. Fragment of microchannel recuperator

In this figure S stands for the radial distance between the hole circles, H is the tangential distance between the holes, D is the diameter of microchannel, L is the thickness of the disk, T is the step of the disks in the recuperator. The calculations of recuperator parameters are presented in Section 8. This recuperator must work with the Ericsson engine shown in the line 2 of Table 1. The engine has very high theoretical efficiency (88% from the corresponding Carnot cycle) but needs low temperature difference (5°C) between hot air and cold air in the recuperator. This temperature difference practically impossible to obtain in heat exchanger that has normal diameters of channels (3-4 mm), but our calculations (Section 8) show that the recuperator with microchannels (with diameter of 0.3 mm) with the temperature difference of 5°C will have acceptable sizes (the diameter of disks of 384 mm and the length of disk stack of 275 mm) for the engine that has power of 10.7kWt. To manufacture this microchannel recuperator it is possible to use MicroEquipment Technology [23]-[25]. In the next section we will describe calculations of microchannels parameters.

VIII. Recuperator Parameters Evaluation

Let us consider microchannel recuperator that has the following dimensions (Fig.20): $D=3\cdot10^{-4}$ m, $S=6\cdot10^{-4}$ m, $H=4\cdot10^{-4}$ m, $L=9\cdot10^{-4}$ m, $T=10^{-3}$ m. The air in different base plates has different temperatures, but for rough estimation of recuperator parameters it is possible to consider the heat transfer process in 2 microchannels (Fig.21) that have mean temperatures:

$$T_{m1} = \frac{T_3 + T_5}{2} = \frac{296+541}{2} = 418.5^\circ K\,, \tag{1}$$

$$T_{m2} = \frac{T_2 + T_4}{2} = \frac{291+536}{2} = 413.5^\circ K\,, \tag{2}$$

where T_{m1} is the mean temperature of expanded (hot) gas, T_{m2} is the mean temperature of compressed (cold) gas, T_2 is the compressed gas temperature at the input of the recuperator, T_4 is the compressed gas temperature at the output of the recuperator, T_3 is the expanded gas temperature at the output of the recuperator, T_5 is the expanded gas temperature at the input of the recuperator. All numerical values of the parameters in the equation (1), (2), and below are drawn from the calculations made for engine version 2 (line 2 in Table 1).

Let us consider the pair or neighbor microchannels (Fig.21).

The channel with the expanded air we will term “hot channel”, and the channel with compressed air we will term “cold channel”. The pressure is the hot channel is:

$$P_{m1} = 2\times10^6\,Pa\,, \tag{3}$$

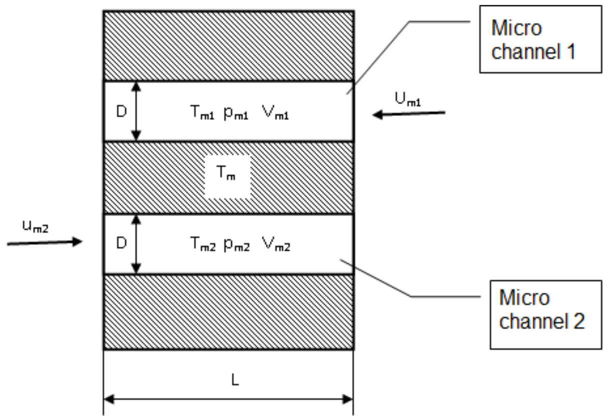

Fig.21. Pair of microchannels

and the pressure in the cold channel is:

$$P_{m2} = 3.45 \times 10^6 \, Pa \, . \quad (4)$$

For our calculations we will suppose that the air speed of compressed air (cold channel) is:

$$u_{m2} = 0.5 \, {}^{m}\!/_{s} \, . \quad (5)$$

The air speed in the hot channel will be higher proportionally to the temperature relation of ${}^{T_{m1}}\!/_{T_{m2}}$ and pressure relation ${}^{P_{m2}}\!/_{P_{m1}}$. So we will have:

$$u_{m1} = u_{m2} \cdot \frac{T_{m1}}{T_{m2}} \cdot \frac{P_{m2}}{P_{m1}} = 0.87 \, {}^{m}\!/_{s} \, . \quad (6)$$

To evaluate the heat transfer process in the microchannel it is possible to use Nusselt number. For laminar flow we accept this Nusselt number:

$$N_u = 3.7 \, . \quad (7)$$

Using this value we can calculate the heat transfer coefficient h that shows how much of heat energy is transferred through 1 square meter of microchannel surface during 1 second if the temperature difference between the wall and the air equals to 1°K:

$$h_1 = h_2 = \frac{k \cdot N_u}{D} \, , \quad (8)$$

where h_1 [W/m$^2 \cdot$ K] is the heat transfer coefficient in the first microchannel, h_2 [W/m$^2 \cdot$ K] is the heat transfer coefficient in the second microchannel, k [W/m$\cdot$ K] is the thermal conductivity of the air, N_u is the Nusselt number, and D is the microchannel diameter. In principle thermal conductivity of the air depends on the temperature, but the difference between the temperatures T_{m1} and T_{m2} is small and it is possible to accept the thermal conductivity coefficient k as equal for two channels. For the temperatures in equations (1) and (2) it will be:

$$k = 0.035 W / m \cdot K \, . \quad (9)$$

The substitution of the values of parameters to the equation (4.8) will give:

$$h_1 = h_2 = 432 W / m^2 \cdot K \, . \quad (10)$$

Mass flow rate in the channel can be obtained from the equation:

$$\varphi_1 = \varphi_2 = \rho_2 \cdot \frac{\pi D^2}{4} \cdot u_{m2} \, , \quad (11)$$

where φ_1 [kg/s] and φ_2 [kg/s] are the mass flow rates in the microchannel 1 and 2, ρ_2 [kg/m^3] is the density of the air in the microchannel 2, D [m] is the microchannel diameter, u_{m2} [m/s] is the mean speed of the air in the microchannel 2.

The density of the air in the microchannel 2 we will calculate using equation:

$$\rho_2 = \rho_0 \cdot \frac{P_{m2}}{P_0} \cdot \frac{T_0}{T_{m2}} \, , \quad (12)$$

where ρ_2 [kg/m^3] is the density of the air in the microchannel 2, ρ_0 [kg/m^3] is the density of the air at the normal conditions (P_0 =102 kPa, T_0 =293°K), ρ_0 =1.2 kg/m^3. From equations (2) and (4) we have T_{m2} =413.5°K and P_{m2} =3.45$\cdot$10^6 Pa. Substitution of these values to (12) gives:

$$\rho_2 = 28.8 \text{ kg/m}^3. \quad (13)$$

Substituting the value ρ_2 from (13) to (11) we obtain:

$$\varphi_1 = \varphi_2 = 1.017 \cdot 10^6 \text{ kg/s}. \quad (14)$$

Now we have to evaluate the heat energy $Q_1[W]$ that is transferred from the air to the walls of microchannel 2 during 1 sec and heat energy $Q_2[W]$ that is transferred from the walls of microchannel 2 to the air. In our case they are equal:

$$Q_1 = Q_2 \, . \quad (15)$$

Due to equal heat energy and equal mass flow rate $\varphi_1 = \varphi_2$

it is evident that the temperature of microchannel walls T_m (Fig.21) will be the following:

$$T_m = \frac{T_{m1} + T_{m2}}{2} = 416^\circ K \ . \tag{16}$$

To calculate the value Q_1 we can use the equation:

$$Q_1 = h_1 \cdot A_1 \cdot (T_{m1} - T_m) \ , \tag{17}$$

where A_1 [m^2] is the area of the walls of the microchannel 1:

$$A_1 = \pi \cdot D \cdot L = 84.8 \cdot 10^{-8} m^2 \ . \tag{18}$$

Substituting the parameter values to (17) we obtain:

$$Q_1 = 9.16 \cdot 10^{-4} W \ . \tag{19}$$

Now we can evaluate decreasing of the air temperature ΔT_{C1} in the microchannel 1 and increasing of the air temperature ΔT_{C2} in the microchannel 2:

$$\Delta T_{C1} = \Delta T_{C2} = \frac{Q_1}{\varphi_1 \cdot C_p} \ , \tag{20}$$

where C_p is the constant pressure heat capacity of the air. For our temperature $C_p = 1014 J / kg \cdot K$.

Substitution parameter values to (20) gives us:

$$\Delta T_{C1} = \Delta T_{C2} = 0.89^\circ K \ . \tag{21}$$

Now we can calculate the number N_d of disks that must contain our recuperator:

$$N_d = \frac{T_5 - T_3}{\Delta T_{C1}} = 275 \ . \tag{22}$$

The number of holes N_h in each disk we can calculate as follows:

$$N_h = 2 \cdot \frac{\varphi}{\varphi_1} \ , \tag{23}$$

where φ [kg/s] is the mass flow rate of the air in the engine and φ_1 is the mass flow rate of the air in the microchannel.

$$\varphi = V_1 \cdot \rho \ . \tag{24}$$

In our calculations we use $V_1 = 0.01 m^3 / s$; $\rho = 24.6 kg / m^3$ at the pressure 20 bar, so we obtain:

$$\varphi = 0.246 kg / s \ . \tag{25}$$

Substitution of the parameter values to the equation (23) gives us:

$$N_h = 484 \cdot 10^3 \ . \tag{26}$$

The whole number of the holes N_R in the recuperator will be:

$$N_R = N_h \cdot N_d = 133 \cdot 10^6 \ . \tag{27}$$

To make this number of the holes it is possible to use microequipment technology described in [23]-[25].

Let us evaluate the diameter of the disk. In Fig.9 we can see that the area a_1 occupied with one hole equals:

$$a_1 = S \cdot H \ , \tag{28}$$

where S[m] is the radial distance between holes and H[m] is the tangential distance between the holes. For diameter of hole of $3 \cdot 10^{-4}$ m it is possible to have $S = 6 \cdot 10^{-4}$ m and $H = 4 \cdot 10^{-4}$ m. In this case:

$$a_1 = 24 \cdot 10^{-8} \text{ m}^2. \tag{29}$$

The area of the disk A_d will be:

$$A_d = N_h \cdot a_1 = 0.116 m^2 \ . \tag{30}$$

The diameter of the disc will be:

$$D_{disk} = \sqrt{\frac{4 \cdot A_d}{\pi}} = 0.384 m \ . \tag{31}$$

The step T of the disks is $1 \cdot 10^{-3}$ m, and the number of disks N_d is 275, so the length L_R of the recuperator is:

$$L_R = T \cdot N_d = 0.275 m \ . \tag{32}$$

Now we can evaluate the air friction energy lost in the recuperator. The volumetric flow rate in the microchannel 1 equals:

$$V_{C1} = \frac{\pi \cdot D^2}{4} \cdot u_{m1} = 6.15 \cdot 10^{-8} m^3 / s \ , \tag{33}$$

and in the microchannel 2 equals:

$$V_{C2} = \frac{\pi \cdot D^2}{4} \cdot u_{m2} = 3.53 \cdot 10^{-8} m^3 / s\,, \tag{34}$$

pressure drop Δp in the microchannel is:

$$\Delta p = \frac{128 \cdot V_C \cdot \mu \cdot L}{\pi \cdot D^4}\,, \tag{35}$$

where V_C [m^3/s] is the volumetric air flow rate, μ [Pa $\cdot$ s] is the dynamic viscosity, L [m] is the channel length, D [m] is the channel diameter.

For $T_m = 416^{\circ} K$ dynamic viscosity

$$\mu = 2.35 \cdot 10^{-5} Pa \cdot s\,. \tag{36}$$

Substitution of parameter values to (35) gives us:

$$\Delta p_1 = 6.54 Pa, \tag{37}$$

$$\Delta p_2 = 3.76 Pa. \tag{38}$$

Power loss in the microchannel is

$$W_0 = \Delta p \cdot V_C\,. \tag{39}$$

For microchannel 1 we will have:

$$W_{C1} = 40.2 \cdot 10^{-8}\, Wt, \tag{40}$$

$$W_{C2} = 13.3 \cdot 10^{-8}\, Wt. \tag{41}$$

The total power loss for air friction in the recuperator W_R will be:

$$W_R = \left(W_{C1} + W_{C2}\right) \cdot \frac{N_R}{2} = 36\, Wt\,. \tag{42}$$

This value is small in comparison with the power of the engine that equals to 10783 Wt (line 2 of Table 1).

IX. Conclusion

We propose new support frame structure for solar concentrator with flat mirrors, discuss the assembly method of the frame structure, and propose the Ericsson heat engine to transfer the heat energy to electrical energy. The Ericsson cycle heat engine can be used to transform heat energy of a solar concentrator to mechanical energy. At present the Stirling cycle and the Rankine cycle are used for this purpose. The problem of these cycles is relatively high temperature difference and relatively low Carnot efficiency. For practically developed Stirling and Rankine heat engines Carnot efficiency reaches 0.6. To obtain good overall efficiency it is necessary to increase the temperature of the concentrator up to 700 C. Special expensive materials are needed to create a heat engine working at such a temperature. If Carnot efficiency is higher, for example 0.8-0.9, the temperature of the solar concentrator can be as low as 400 C. This temperature permits us to make heat engines from low cost materials. For Ericsson engine the temperature of the solar concentrator can be as low as 400 C. This temperature permits us to make heat engines from low cost materials. A special computer program was developed for estimation of parameters for the Ericsson cycle heat engine. Experiments with this program show that Ericsson cycle can have Carnot efficiency up to 0.88.

Microchannel recuperator for Ericsson heat engine is proposed. This recuperator has the volume about 32 liters and permits us to create the Ericsson engine with power of some kWts. The recuperator contains $133 \cdot 10^6$ microchannels (holes). It is necessary to have micromachine technology to produce this type of recuperator. This technology was proposed in or previous works.

Acknowledgment

We thank L.R. Vega González, E. Camacho Corona, G. González González, and I.J. Hernández Jardinez for fruitful discussions of our investigation in area of solar concentrators with flat mirrors and their assistance in patent application.

References

[1] R. Snow, M. Snow, “Transitioning to a Renewable Energy Economy,” in Proc. *WSEAS Recent Researches in Environmental & Geological Sciences*, Kos Island, Greece, July 14-17, 2012, pp.62-67.

[2] D. Wood, “Matrix solar dish,” US patent N°6485152, 2002.

[3] A. Lewandowskj, et al., “Multi-facet concentrator of solar,” US patent N°6225551, 2001.

[4] E. Kussul, T. Baidyk, O. Makeyev, F. Lara-Rosano, J. M. Saniger, N. Bruce, “Development of Micro Mirror Solar Concentrator, ” in *Proc. 2-nd IASME/WSEAS Intern. Conf. on Energy and Environment (EE’07)*, Portoroz (Portotose), Slovenia, May 15-17, 2007, pp.294-299.

[5] E. Kussul, T. Baidyk, F. Lara-Rosano, J. Saniger, N. Bruce, “Support Frame for Micro Facet Solar Concentrator,” in *Proc. 2-nd IASME/WSEAS Intern. Conf. on Energy and Environment (EE’07)*, Portoroz (Portotose), Slovenia, May 15-17, 2007, pp.300-304.

[6] G. Johnston, “Focal region measurements of the 20 m^2 tiled dish at Australian National University,” Solar Energy, Vol.63, No.2, pp. 117-124, 1998.

[7] http://www.anzses.orglGallery/Dish.html The Australian and New Zealand Solar Energy Society, White Cliffs Dish — 20 m^2 dish at ANU.

[8] E. Kussul , T. Baidyk , O. Makeyev, F. Lara-Rosano, J. Saniger., N. Bruce, “Flat facet parabolic solar concentrator with support cell for one and more mirrors, ” *WSEAS Trans. on Power Systems*, Issue 8, Vol.3, August 2008, pp.577-586.

[9] E. Kussul, T. Baidyk, F. Lara, J. Saniger, N. Bruce, C. Estrada, “Micro facet solar concentrator,” *Intern. J. of Sustain. Energy*, 2008, Vol.27, Issue 2, pp.61-71.

[10] http://bbxinhua.en.made-in-china.com/product/UMNJgpdjEFhx/China-4mm-Frameless-Float-Glass-Mirror-Reen-lu-20-.html

[11] D. Wood, “Support structure for a large dimension parabolic reflector and large dimension parabolic reflector,” EP 0022887 A1 (D. Wood) 21.12.1983 (24.07.1979)

[12] Estufa solar para poblaciones urbanas, Centro de Investigación y Estudios Avanzados (Cinvestav) Mexico, http://pepegrillo.com/2009/02/estufa-solar-para-poblaciones-urbanas/

[13] E.Kussul, T. Baidyk, F. Lara-Rosano, J. Saniger, G. Gasca, N. Bruce, “Method and device for mirrors position adjustment of a solar concentrator,” US Patent Application 20110215073, 2.03.2011

(MX/A/2010/002418 MX 03/02/2010)
[14] Bancha Kongtragool, Somchai Wongwises, "A review of solar-powered Stirling engines and low temperature differential Stirling engines," Renewable and Sustainable Energy Reviews, 7, 2003, pp.131–154.
[15] American Stirling Company (beautiful Stirling engines and kits), http://www.stirlingengine.com/
[16] Koichi Hirata, Schmidt theory for Stirling engines, 1997, http://www.bekkoame.ne.jp/~khirata/academic/schmidt/schmidt.htm
[17] Bancha Kongtragool, Somchai Wongwises, "Performance of low temperature differential Stirling engines," Renewable Energy, 32, 2007, pp.547-566.
[18] Jincan Chen, Zijun Yan, Lixuan Chen and Bjarne Andresen, "Efficiency bound of a solar-driven Stirling heat engine system," *Int. J. Energy Res*., 22, 1998, pp.805-812.
[19] L. Berrin Erbay, Hasbi Yavuz, "Analysis of an irreversible Ericsson engine with a realistic regenerator," *Appl. Energy*, Vol. 62, Issue 3, March 1999, pp.155–167.
[20] S. Bonnet, M. Alaphilippe, P. Stouffs, "Energy, exergy and cost analysis of a micro-generation system based on an Ericsson engine," *Intern. J. Thermal Sci.*, 44, 2005, pp.1161-1168.
[21] E. Kussul, T. Baydyk, "Thermal motor for solar power plants," in *Proc. 3er Congreso Internacional de Ciencias, Tecnología, Artes y Humanidades*, 3-6 de junio 2009, Coatzacoalcos, Veracruz, México, pp. 684-688.
[22] L. Ruiz-Huerta, A.Caballero-Ruiz, G. Ruiz, G. Ascanio, T. Baydyk, E. Kussul, R. Chicurel, "Diseño de un motor de ciclo Ericsson modificado empleando energía solar," in *Proc. Congreso de Instrumentación SOMI XXIV*, Mérida, Yucatán, México, 14-16 de Octubre de 2009, pp.1-7.
[23] E. Kussul, D. Rachkovskij, T. Baidyk, S. Talayev, "Micromechanical engineering: a basis for the low-cost manufacturing of mechanical microdevices using microequipment," *J. Micromechanics& Microengineering*, 6, V.6, 1996, pp. 410-425.
[24] E. Kussul, T. Baidyk, L. Ruiz-Huerta, A. Caballero, G. Velasco, L. Kasatkina, "Development of micromachine tool prototypes for microfactories," *J. Micromechanics&Microengineering*, **12**, 2002, pp. 795-813.
[25] E. Kussul, T. Baidyk, D. Wunsch, *Neural Networks and Micromechanics*, Springer, 2010, pp.210.

Ernst M. Kussul (Ph.D.'67). From 1967 till 1998 he worked in the Institute of Cybernetics of Ukrainian Academy of Sciences. In 1982 he received the D. Sci. degree in artificial neural networks. From 1988 to 1998 he was Head of the Department of Neural Networks in the International Research and Training Center of UNESCO/IIP of Information Technologies and Systems. Since 1998 he is Researcher level "C" in UNAM, Mexico.

He is author and coauthor more than 200 publications, 4 books, 11 patents. His present research interests are micromechanics, mechatronics, neural networks, and pattern recognition.

Dr. Kussul is a member of IEEE. He is a member of the Mexican Academy of Sciences and National System of Scientists.

Oleksandr Makeyev (AM'05,Ph.D.'10) received B.S. in mathematics and M.S. in statistics from National Taras Shevchenko University of Kyiv, Kiev, Ukraine, in 2003 and 2005 respectively. He received his Ph.D. in 2010 from the Department of Electrical and Computer Engineering, Clarkson University, Potsdam, USA and worked there as a Research Assistant. Now he works as Postdoctoral Fellow in Department of Electrical, Computer, and Biomedical Engineering, University of Rhode Island, Kingston, USA.

He has more than 20 publications. His research interests include neural networks, pattern recognition, evolutionary computation, wavelets and time series analysis.

Dr.Makeyev is a member of IEEE.

Tatiana N. Baidyk (Ph.D'83). From 1977 to 1995 she was with the Institute of Cybernetics of the Ukrainian Academy of Sciences. In 1994 T.Baidyk received D.Sci. in the area of neural networks. From 1995 to 1999 she was coordinator of the International Program of Education and Science in Ukraine, International Renaissance Foundation. From 1998 she was with the International Research and Training Center of UNESCO/IIP of Information Technologies and Systems as a leading researcher. From 2001 till now she has been Researcher in UNAM, Mexico.

She has near 200 publications, 3 books, 3 patents. Baidyk´s present research interests are neural networks, pattern recognition, control systems, and industrial applications.

Dr. Baydyk is a member of the Mexican Academy of Sciences and National System of Scientists.

Jose Saniger Blesa(Ph.D.88) He received his Ph.D. from University Complutense, Madrid, Spain in 1988. He worked in Laboratory of Chemistry of Materials, UNAM. Actually he works in Group of Materials and Nanotechnology in CCADET, UNAM and he is Director of CCADET, UNAM.

He has more than 80 publications in international journals, 5 chapters in books. He has scientific interests in solid state chemistry, materials synthesis and characterization, nanostructures of materials, development of catalysts based on nanoparticles with gold, etc. He is the principal coordinator of University Project in Environment Nanotechnology.

Dr. Saniger is the President of Mexican Society of Instrumentation and regular member of Mexican Academy of Sciences, American Chemistry Society, and American Association for the Advancement of Science.

Neil Bruce(B.Sc.87, M 88, Ph.D.92) received B.Sc. with Honors in Physics in the University of Edinburgh in Scotland in 1987, and Master degree in Applied Optics and Ph.D. in Physics in Imperial College, London in 1988 y 1992, respectively.

He published over 30 articles in international journals and participated in 15 international conferences. His interests are measurement and simulations of light scattering on rough surface with application in medicine and in characterization of rough surfaces.

Dr. Bruce is member of National System of Scientists.